

Document downloaded from:

<http://hdl.handle.net/10251/62441>

This paper must be cited as:

Climent Olmedo, M.J.; Corma Canós, A.; Hernández, J.C.; Hungría, A.B.; Iborra Chornet, S.; Martínez Silvestre, S. (2012). Biomass into chemicals: One-pot two- and three-step synthesis of quinoxalines from biomass-derived glycols and 1,2-dinitrobenzene derivatives using supported gold nanoparticles as catalysts. *Journal of Catalysis*. 292:118-129. doi:10.1016/j.jcat.2012.05.002.



The final publication is available at

<http://dx.doi.org/10.1002/cplu.201500042>

Copyright Elsevier

Additional Information

Biomass into chemicals: One-pot two and three steps synthesis of quinoxalines from biomass derived glycols and 1,2-dinitrobenzene derivatives using supported gold nanoparticles as catalysts.

M. J. Climent^a, A. Corma^{a*}, J. C. Hernández^b, A. B. Hungría^b, S. Iborra^{a*}, S. Martínez-Silvestre^a

^a *Instituto de Tecnología Química (UPV-CSIC).*

Universidad Politécnica de Valencia. Consejo Superior de Investigaciones Científicas.

Avenida de los Naranjos s/n, 46022, Valencia, Spain.

^b *Departamento de Ciencia de los Materiales e Ingeniería Metalúrgica y Química*

Inorgánica. Universidad de Cádiz (UCA).

Carpas Río San Pedro s/n, 11510, Puerto Real, Cádiz, Spain.

*** To whom correspondence should be addressed**

| | | |
|----------------------|---------------|--|
| Avelino Corma | E-mail | acorma@itq.upv.es |
| | Fax: | (+34) 963877809 |
| | Phone: | (+34) 963877800 |
| Sara Iborra | E-mail | siborra@itq.upv.es |
| | Phone: | (+34) 963877840 |

Abstract

An efficient and selective one-pot two steps, method for the synthesis of quinoxalines by oxidative coupling of vicinal diols with 1,2-phenylenediamine derivatives, has been developed by using gold nanoparticles supported on nanoparticulated ceria (Au/CeO₂) or hydrotalcite (Au/HT) as catalysts and air as oxidant, in absence of any homogeneous base. Reaction kinetics shows that the reaction controlling step is the oxidation of the diol to α -hydroxycarbonyl compound. Furthermore, a one-pot three steps synthesis of 2-methylquinoxaline starting from 1,2-dinitrobenzene and 1,2-propanediol has been successfully carried out with 98% conversion and 83% global yield to the final product.

Keywords: cascade process, quinoxaline, 2-methylquinoxaline, Au/CeO₂, Au/HT, heterogeneous catalyst, 1,2-phenylenediamine, diol, biomass.

1. Introduction

In the last decade the research of renewable reactants has become a key issue for a sustainable chemistry [1-5]. Approximately 75% of the biomass produced by Nature through the process of photosynthesis corresponds to carbohydrates, but only between 3-4% of these compounds are used for food and non-food purposes [6]. Therefore the use of carbohydrates as raw materials for the production of basic chemicals is an area of increasing interests [7-11]. In this sense, a variety of glycols (1,2-ethanediol, 1,2-propanediol, 1,2-butanediol or 2,3-butanediol) can be obtained from carbohydrates [1-5,12] as well as from glycerol [13,14] via bio- or chemocatalytic reactions. Those glycols could be used as starting reactants to obtain products with higher added value.

The aim of the present work is to obtain quinoxalines starting from glycols derived from biomass and 1,2-phenylenediamine or 1,2-dinitrobenzene derivatives, through a cascade reaction process. Quinoxalines, also called benzopyrazines, and their derivatives show a broad spectrum of biological activity including antitumor [15], antiviral [16], antituberculosis [17], anti-inflammatory [18,19], anti-protozoal, anti-HIV [20,21], and have been evaluated as anticancer and anthelmintic agents [22]. Quinoxaline moieties, have also found applications as dyes [23], cavitands [24], efficient electroluminescent materials [25], building blocks in the synthesis of organic semiconductors [26], chemically controllable switches [27] and dehydroannulenes [28].

Quinoxaline synthesis is conventionally carried out by a double condensation between 1,2-phenylenediamines and 1,2-dicarbonyl compounds [29-33]. However, the handling of highly reactive dicarbonyl compounds is an important drawback. Other synthesis methods involving 1,4-addition of 1,2-diamines to diazenylbutenes [34], oxidation-trapping of α -hydroxycarbonyl compounds with 1,2-diamines [35-38], cyclization–oxidation of phenacyl bromides and 1,2-phenylenediamines through solid-

phase synthesis [39] and oxidative coupling of epoxides with ene-1,2-diamines [40] have been developed for the synthesis of substituted quinoxalines. Unfortunately, most of these methods suffer from unsatisfactory yields, difficult experimental procedures, the use of expensive and detrimental metal precursors, or demanding reaction conditions. Therefore, there is a clear incentive to develop catalytic process able to produce the quinoxalines by environmentally friendly methods, while minimizing the number of reaction steps through a more intensive one pot type catalytic process.

In this sense, an elegant alternative to the previously reported methods could be a cascade process in where the vicinal diols are oxidized and the resulting α -hydroxycarbonyl or 1,2-dicarbonyl compound goes to a cyclocondensation with 1,2-phenylenediamines. This approach has been followed by Cho et al. [41], using $\text{RuCl}_2(\text{PPh}_3)_3$ as homogeneous catalyst (phenylenediamine derivative/catalyst molar ratio of 50) together with large amounts of KOH (KOH/phenylenediamine derivative molar ratio of 4), in reflux of diglyme (5 mL), to reach 70-80% yield of the corresponding quinoxaline derivatives.

In recent years, heterogeneous catalysts have gained more importance due to environmental and economic factors, and uni or multisite solid catalysts have been successfully used for process intensification and waste minimization in several organic transformations [42-45]. Thus, the synthesis of 2-methylquinoxaline with solid catalysts was performed by Gopal et al. [46] with transition metals (Pb, Cu, Mn and Cr) and La supported on HY zeolite at 350 °C, and 82% yield of 2-methylquinoxaline was achieved with a Pb/HY catalyst. Others [47] have performed the photocatalytic synthesis at room temperature over TiO_2 /zeolite (HY, HBeta or HZSM-5) with a maximum yield of 22% for 2-methylquinoxaline over 5 wt% of TiO_2 /HBeta catalyst. While the above reports

offer interesting perspectives, they require higher temperatures, the selectivity is low or the process involves large amounts of a base that has to be neutralized.

In early work about heterogeneous catalytic oxidation of alcohols, supported palladium and platinum catalysts with metal promoters such as bismuth or lead were intensively investigated [48], while low-valent ruthenium species were also known to be excellent catalysts for the dehydrogenation of alcohols [49]. Recently, gold in the form of nanoparticles has been recognized as a promising metal for the aerobic oxidation of alcohols in the absence of base and under mild reaction conditions [50,51].

Taking into account the above, we thought that it should be now possible to carry out the synthesis of quinoxalines by performing the oxidation of diols to the carbonyls and the following cyclocondensation with 1,2-phenylenediamines derivatives in a one-pot two steps synthesis under very mild reaction conditions (see Scheme 1).

Herein we present that gold nanoparticles supported on different carriers are able to catalyse, with high selectivity, the one-pot synthesis of quinoxalines from vicinal diols and 1,2-phenylenediamines derivatives under base free conditions (Scheme 1). Moreover it will also be shown that with the gold catalyst, the process can also be extended to a new one-pot three steps synthesis using diols and the directly accessible 1,2-dinitrobenzene reactant (Scheme 2).

2. Experimentals and methods

2.1. Synthesis of catalysts

Synthesis of Au/CeO₂ catalysts: Gold was supported on cerium oxide nanoparticles [52] with a BET surface area of 180 m²·g⁻¹. Gold was deposited on the nanoparticulated ceria by using the following procedure. A solution of H₂AuCl₄·3H₂O (700 mg) in deionised water (160 mL) was brought to pH = 10 by addition of a solution of NaOH

0.2 M. Once the pH value was stable the solution was added to a solution containing CeO₂ (4.01 g) in H₂O (50 mL). After adjusting the pH of the slurry at a value of 10 by addition of a NaOH 0.2 M solution, the slurry was continuously stirred vigorously for 18 h at room temperature. The Au/CeO₂ solid was then filtered and exhaustively washed with distilled water until no traces of chlorides were detected by the AgNO₃ test. After that, the supported gold nanoparticles were reduced with 10 mL of 1-phenylethanol, at 160 °C, during two hours under constant agitation. The catalyst was washed with water and acetone and dried under vacuum at room temperature for 1 h. The total Au content of the final catalyst was 4.5 wt% as determined by chemical analysis. The metal particle size was determined by High Angle Annular Dark Field Scanning Transmission Electron Microscopy (HAADF-STEM), and images were acquired with a JEOL 2010 field emission gun transmission electron microscope operated at 200 kV equipped with a X-EDS Oxford Inca Energy 2000 system.

Synthesis of Au/HT catalysts: The Al/Mg hydrotalcite (HT) support was prepared by co-precipitation of two salts containing Al⁺³ and Mg⁺² [53]. The synthesis is performed at constant pH, by slow addition, in a single container, of two diluted solutions (A and B), namely, solution A containing Mg(NO₃)₂·6H₂O and Al(NO₃)₃·9H₂O, 1.5 M in (Al+Mg) with Al/(Al+Mg) atomic ratio equal to 0.25, and solution B prepared by dissolving Na₂CO₃ and NaOH in water in such way that the ratio CO₃²⁻/(Al + Mg) is equal to 0.66. Both solutions were co-added at a rate of 1 mL·min⁻¹ under vigorous mechanical stirring at room temperature. The gel was aged under autogeneous pressure conditions at 333 K for 12 h. Then, the hydrotalcite was filtered and washed until pH = 7 and the solid was dried.

To prepare an Au/HT catalyst, the obtained HT (1.0 g) was added to 50 mL of an aqueous solution of HAuCl₄ (2 mM). After stirring for 2 min, 0.09 mL of aqueous NH₃

(10% v/v) was added and the resulting mixture stirred at room temperature for 12 h. The obtained slurry was filtered, washed with deionised water, and dried at room temperature in vacuo. Subsequent treatment with H₂ (flow = 90 mL·min⁻¹) at 180 °C for 3h, gives Au/HT sample as a purplish red powder. The Au loading on Au/HT was found to be 0.7 wt% by elemental analysis. Another catalyst was prepared in where the original HT support was calcined at 450 °C in a N₂ flow for six hours to produce the mixed oxides before 0.7 wt% gold was supported following the same procedure than above. The resultant catalyst is named Au/HTcalc.

Synthesis of Au/MgO catalyst: A nanoacrySTALLINE MgO support ($\geq 600 \text{ m}^2\cdot\text{g}^{-1}$ BET surface area) was purchased from NanoScale Materials Inc. The synthesis of Au/MgO sample was carried out from MgO and an aqueous solution of HAuCl₄, following the method described for Au/HT. Chemical analysis gave 0.6 wt% Au on the catalyst.

1.5 wt% Au/TiO₂ and 4.5 wt% Au/Fe₂O₃ catalysts: These samples were directly purchased from TEK and WGC respectively and they were used as received.

2.2. Reagents

All reagents were purchased from Sigma Aldrich except Au(CH₃)₂(acac) which was purchased from Strem, and 4-methoxybenzene-1,2-diamine which was synthesized from 4-methoxy-2-nitroaniline by hydrogenation of the nitro group over Au/TiO₂ [54].

2.3. Catalyst regeneration and reuse

For catalyst reuse, the catalyst after reaction was collected by vacuum filtration and then it was repeatedly washed. First, it was washed with diethyl ether to remove organic compounds, subsequently it was washed with NaOH (0.2 mol·L⁻¹) to remove any acid byproducts that may poison the gold nanoparticles. Then water was used to

remove traces of NaOH on the catalyst, and at last the catalyst was washed with diethyl ether again. Finally, the catalyst was dried overnight and then it is ready for reuse.

2.4. Reaction procedure

A generic experiment was as follows. In a two-neck round bottom flask of 10 mL, 1,2-phenylenediamine (**1a**, 0.5 mmol), 1,2-propyleneglycol (**2a**, 0.6 mmol), 1.5 mL of diethylene glycol dimethyl ether (diglyme) and an amount of catalyst were added. Subsequently the reaction mixture was heated at 140 °C in a silicone bath that contains a magnetic stirrer and a temperature controller. In another series of experiments the same methodology was followed, but some of the reaction conditions were changed in order to see the effect of temperature, diamine/Au ratio, catalyst loading and oxygen pressure.

For the one-pot three steps experiment, the reaction was performed using 0.5 mmol of 1,2-dinitrobenzene, 0.6 mmol of **2a**, 10.5 mmol of diglyme and 20 mg of Au/CeO₂ (4.5 wt%) as catalyst.

The progress of the reaction was followed by taking samples at regular time periods and analyzing them by gas chromatography using a FID detector and a capillary column (HP5, 30 m × 0.25 mm × 0.25 μm). All samples were dissolved in ethyl acetate prior to analysis by gas chromatography. Nitrobenzene was used as the external standard. At the end of the reaction the catalyst was filtered and washed according to the regeneration of the catalyst section. The extract is concentrated and quantified in the final outcome of the reaction and the catalyst is ready to be reused. In all cases the total final mass of the reaction (including the filtered extract) was over 90% of the initial amount weighed.

The products obtained were characterized by ¹H-RMN (300 MHz Bruker Avance). The content of organic (wt% C, H, N, S) was measured by elemental analysis with an EA-1108 CHNS Fisons analyzer and sulphanilamide as standard. The

thermogravimetric analyses were carried out with a TGA 2050 by TA Instruments, under an air flow and with a heating rate of $10 \text{ K}\cdot\text{min}^{-1}$. Mass spectra were performed by GC-MS (HP Agilent 5988 A with a 6980 mass selective detector).

3. Results and discussion

3.1. Reaction network

Following the general reaction procedure previously explained and using Au/CeO₂ as catalyst, the reaction between 1,2-phenylenediamine (**1a**) and 1-phenylethane-1,2-diol (**2g**) (Scheme 3) was followed with time, and the kinetic curves are given in Figure 1 (see also Scheme 4). At the beginning of the reaction, only the α -hydroxycarbonyl compound (**4**), formed by oxidation of the diol **2g**, and benzaldehyde (**6**) which comes from the oxidative cleavage of **2g** were observed as primary products. However, after one hour reaction, their concentration decreases probably by reaction of the α -hydroxycarbonyl compound (**4**) with a molecule of phenylenediamine **1a** to afford 2-phenylquinoxaline **3** and, in a much lesser degree, the benzimidazole derivatives (**8**, **9**, **10** and **11**) [55]. Since this consecutive reaction is very fast, product **3** appears as a pseudo primary product. The dicarbonyl compound (**5**), produced by oxidation of α -hydroxycarbonyl compound **4**, was detected at trace level, and the formaldehyde (**7**) produced by oxidative cleavage of the diol was not detected. This behaviour allows us to consider that the α -hydroxycarbonyl compound **4** is a primary and unstable product and dicarbonyl compound **5** is a secondary and unstable product.

Taking into account the kinetic behaviour of the different compounds presented in Figure 1, a reaction network is presented in Scheme 5, in where the diol **2** is firstly oxidized to the α -hydroxycarbonyl compound **4** and subsequently to the dicarbonyl compound **5**. Both compounds can condensate with the diamine **1** to produce the imine

intermediates **13** and **14** (non-detectable by GC), being **13** converted into product **14** by a fast oxidation of the remaining hydroxyl group. Finally, product **14** follows the condensation to yield quinoxaline **3**. Additionally, we have reacted 2-hydroxy-1-phenylethanone **4** and 2-oxo-2-phenylacetaldehyde **5** under the same reaction conditions. Then, from the results given in Table 1, one can see that when starting from **2g**, the reaction is slower than when the reaction started from α -hydroxycarbonyl compound **4**. Moreover, when we fed dicarbonyl compound **5** the reaction was very fast. From these results we can conclude that the controlling reaction step in the process should be the oxidation of compound **2** into compound **4**.

Interestingly we found that when the reaction started from diol **2g** or α -hydroxycarbonyl compound **4**, the same type of by-products (**6**, **8** and **9**) were detected, while in the experiment starting with dicarbonyl compound **5**, no by-products were observed. These results show that the by-products detected are produced from the oxidative cleavage of the diol and/or the hydroxycarbonyl compound **4** into the aldehydes **6** and **7**. Later, products **6** and **7** condensate with phenylenediamine **1** giving the benzimidazole derivatives **8**, **9**, **10** and **11**.

3.2. Reactivity of the different metal supported catalysts

In order to determine the possibilities of gold as a catalyst for the synthesis of quinoxalines, the catalytic activity of different gold supported catalysts were studied for the reaction of 1,2-phenylenediamine (**1a**) with the 1,2-propanediol (**2a**) to obtain 2-methylquinoxaline (**3a**) (Scheme 6). Thus, the reaction was carried out in diglyme as a solvent at 140 °C in presence of gold supported on: CeO₂ nanoparticles, TiO₂, Fe₂O₃, MgO, HT and calcined HT (HTcalc). Regardless of the support used, gold was active and selective for the above mentioned reaction (Table 2) and, in all cases, the main by-

products detected were 2-methyl-1*H*-benzo[d]imidazole (**8**) and 1-*H*-benzo[d]imidazole (**9**) which are produced from the oxidative cleavage of 1,2-propanediol giving the corresponding aldehydes, followed by condensation with 1,2-phenylenediamine (see Scheme 5).

In a first approximation, we have checked if the differences in activity observed among the different catalysts can be due to difference in metal particle size. Then the number of external surface atoms was calculated for each catalyst on the basis of the mean particle size, and with this value and initial reaction rates, a turnover frequency (TOF) was calculated for each catalyst. According to the TEM images, the shape of gold nanoparticles looks predominantly cubic. Thus by assuming this crystal shape, the number of particle gold atoms (N_T) was calculated according to Equation (1), in which $\langle d \rangle$ corresponds to the mean diameter of gold particles as determined experimentally by TEM and d_{at} is the atomic diameter of gold (0.288 nm). Considering that in the face centered cubic (fcc) crystal one atom is surrounded by twelve others assuming a full shell close packing model and N_T is related to the number of shells (m) [Eq. (2)], then the number of external atoms (N_S) can be calculated with Equation (3) [56,57].

$$N_T = \frac{10m^3 - 15m^2 + 11m - 3}{3} \quad (1)$$

$$\langle d \rangle = 1.105 \cdot d_{at} \cdot \sqrt[3]{N_T} \quad (2)$$

$$N_S = 10m^2 - 20m + 12 \quad (3)$$

As can be seen in Table 2 and Figure 2, Au/CeO₂ and Au/HT catalysts present the highest activity (TOF values) among the different gold catalysts tested, achieving conversions >85% with high selectivities (entries 1 and 2). Meanwhile Au/TiO₂, Au/Fe₂O₃, and Au/MgO catalysts (entries 3, 4 and 5), that are active for different oxidation and reduction reaction, show much lower activity at a similar number of gold

surface atoms than Au/CeO₂ and Au/HT. The influence of the support on the rate of alcohol oxidation by gold has been attributed to changes produced on the crystallite shape as well as to the participation of the support in the catalytic cycle [58,59]. In the case of CeO₂, it has been reported that surface saturation by O₂ is already achieved at relatively low partial pressure of O₂, as could be expected due to the excellent capacity of CeO₂ to act as an oxygen pump due to the presence of surface oxygen vacancies that arises from the small size of ceria nanoparticles [60-62]. Otherwise, HT has a structure of brucite-like layers containing octahedrally coordinated cations of Mg²⁺ and Al³⁺ as well as interlayer anions (CO₃²⁻ and OH⁻ mainly) which has been reported as an excellent catalyst for alcohol oxidation that form Au-alcoholate species [63-66] due to the basic surfaces of HT. However, when HT support is calcined, the layered structure disappears and a mixed Al₂O₃-MgO oxide is formed that presents stronger basicity than the starting hydrotalcite [67]. Then when gold is deposited, the results in Table 2, entry 6, show a lower TOF for gold on the mixed oxides than the gold on hydrotalcite (entry 2). In spite of the acceptable activity of the Au/HTcalc (entry 6), the conversion achieved after 24 hours of reaction is considerably lower than with Au/HT catalyst. As can be observed in Figure 2, a strong deactivation occurs with this catalyst. This behaviour can be attributed to the existence of strong basic sites on the support, which could promote the strong adsorption of the weak acidic diol giving the deactivation of the catalyst. In fact, when MgO was used as support, and despite its large surface area ($\geq 600 \text{ m}^2\cdot\text{g}^{-1}$), the average crystallite size of supported gold is larger and gives low activities and selectivities. It appears then, that some basicity of the support and high metal dispersion (small gold nanoparticles) would be positive for the reaction. Notice that when the reaction was carried out with the supports (CeO₂ and HT) without gold, the yields to product **3a** were much lower (Table 2, entries 7 and 8), whereas no

products were detected in absence of catalyst. Therefore, if one takes into account that the controlling step for the reaction is alcohol oxidation, it appears clear that smaller gold nanoparticles supported on carriers with mild basicity and carriers able to adsorb large amount of oxygen should be adequate catalyst for the one-pot two steps synthesis of quinoxalines.

3.3. Stability and reusability of Au/CeO₂ and Au/HT catalysts

Catalyst recyclability was checked by performing successive reuses of the catalyst under the same reaction conditions. To do that, the catalyst recovered, as explained in the experimental section, was used in a subsequent run. The results of Au/CeO₂ catalyst recycling are shown in Figures 3 and 4. As can be seen there, Au/CeO₂ catalyst slowly deactivates with use.

In order to check if deactivation was due to gold leaching and the leached gold was the main responsible for activity, the reaction was performed under the same conditions, and after 2 hours the gold catalyst was removed by filtration, being the reaction continued with the filtrate. Under these conditions, no further conversion was observed (Figure 5). In addition, no traces of gold were detected in the reaction filtrate. Furthermore, the gold content in the used catalyst was determined by X-ray fluorescence, and no changes were detected with this technique after four runs. These results indicate that deactivation of the catalyst after four runs is not due to gold leaching from the support. A TG analysis of the used Au/CeO₂ sample showed that 5 wt% of organic material remains on the catalyst after the first use, which increases up to 14 wt% after the third use. Therefore, it may very well occur that the organic deposited on the catalyst surface could be the cause of catalyst deactivation. Then, in a new recycling experiment, after the third use the catalyst was treated in air at 300 °C for 10

hours. After calcination, the organic content of the catalyst was reduced from 14 to 3 wt%. When this catalyst was used again in the reaction, it was observed that, although some of the activity was recovered, the activity was still lower than for the fresh catalyst (see Figure 3 and cycle 4 in Figure 4). The lower activity of the regenerated catalyst could be explained by an increase in the size of gold nanoparticle due to metal agglomeration occurring during calcination. To check this possibility, the metal crystal size was determined by TEM for the used catalyst, and the results from Figure 6, clearly show that crystal agglomeration occurs during calcination. Finally to address the deactivation issue we have also considered a potential loss of activity due to the presence of carboxylic acids [68] which could be formed by deep oxidation of the diol and that act as poison for gold. To check that possibilities, an experiment was carried in the presence of KOH to avoid acid deposition on the catalyst, but a significant decrease of the selectivity to 2-methylquinoxaline was observed (64% at full conversion). Therefore we believe that catalyst deactivation during reaction mainly occurs by “coking”, but by burning off the organic deposits provided that metal sinterization is avoided. Therefore catalyst regeneration for this process needs to be explored more deeply.

Similar results were obtained during the recycling of Au/HT catalyst (see Figure 7), i.e. the catalyst deactivates, but leaching of gold was not detected. However, catalyst calcination at 300 °C does not restore but further decreases activity (cycle 4, Figure 8), this is probably due (see Figure 9) to an increase of the basicity of the support due to the calcination treatment, which agrees with the results previously presented in Table 2, entry 6.

3.4. Optimization of reaction conditions: diamine/Au ratio, temperature, catalyst Au loading and oxygen pressure

Taking into account activity, selectivity, regenerability, and performance of the catalyst, we have selected Au/CeO₂ as the catalyst to synthesize quinoxalines, and the influence of reaction conditions on conversion and selectivity has been studied. Firstly the conversion to 2-methylquinoxaline with reaction time was followed using Au/CeO₂ and working at reactant to gold molar ratio of 100, 200 and 400 (see Table 3). The initial reaction rate is directly proportional to the concentration of the catalyst, and as can be observed in Table 3 (entries 1, 2 and 3) > 95% conversion of **1a** can already be achieved with 1% molar catalyst loading.

The influence of the temperature (100 °C, 120 °C, 140 °C and 160 °C) on the reaction rate, working at 1 mol% Au content, is shown in Table 3 (entries 3, 4, 5, and 6). As can be expected, when increasing the temperature an increase of the reaction rate is observed, while selectivity to **3a** decreases at temperature higher than 140 °C owing to the oxidative cleavage of the glycol which is more favoured when increasing the reaction temperature (see Figure 10). Therefore 140 °C was selected as an optimum reaction temperature.

The influence of oxygen partial pressure was studied by performing the reaction while continuously bubbling O₂ (Table 3, entry 7), or by working in a closed reaction system under 3 bars of air or O₂ (entries 8 and 9). The results obtained indicate that while the rate of the reaction does not increase when increasing oxygen partial pressure, the selectivity to 2-methylquinoxaline decreases due to an increase in the production of benzimidazole derivatives. This is due to the fact that at higher oxygen partial pressure, the oxidative cleavage of the glycol is favoured (see Scheme 5).

3.5. Scope of the reaction

Under optimized reaction conditions, we have analyzed the possibility to perform the one-pot, two steps preparation of quinoxaline derivatives with Au/CeO₂ starting from several diols (1,2-ethanediol **2b**, 2,3-butanediol **2c**, 1,2-butanediol **2d**, 1,2-pentanediol **2e**, 1,2-hexanediol **2f**, 1-phenylethane-1,2-diol **2g** and *m*-hydrobenzoin **2h**) and **1a**, and the results are given in Table 4. As can be seen there, conversion and selectivity to the corresponding quinoxalines were excellent except in the case of diols with aromatic substituent (**2g** and **2h**), which were more prone to undergo the oxidative cleavage.

The influence of different substituents in position 4 of 1,2-phenylenediamine (4-nitrobenzene-1,2-diamine **1b**, 4-chlorobenzene-1,2-diamine **1c**, 3,4-diaminobenzonitrile **1d**, 4-methylbenzene-1,2-diamine **1e**, naphthalene-2,3-diamine **1f**, 4-methoxybenzene-1,2-diamine **1g**) on the reaction rate and product selectivity for the oxidation-cyclization process of 1,2-ethanediol (**2b**), was studied in presence of Au/CeO₂. As can be seen in Table 5, good yields to quinoxaline derivatives are obtained in all cases. However, when electron withdrawing substituent such as, nitro, chloride or nitrile groups are presents, quinoxaline derivatives yields are lower with respect to 1,2-phenylenediamine (Table 5, entries 1-4), or with respect to phenylenediamine molecules with electron-donating substituents like methyl, (-CH₂)₄ or methoxy groups (Table 5, entries 5-7). Similar results have been described in the literature for the reaction between α -hydroxycarbonyl compounds and 1,2-phenylenediamine derivatives [31, 35 and 37].

3.6. One-pot three steps, synthesis of quinoxalines

Owing to the success of Au/CeO₂ for catalyzing the oxidation-cyclization of 1,2-diamines with 1,2-diols, and taking into account the gold ability for chemoselective

reduction of nitro to amino groups [54,69-71], we have attempted a one pot three steps process which involves the reaction between 1,2-dinitrobenzene **15** and 1,2-propanediol **2a** to achieve the one-pot synthesis of 2-methylquinoxaline as shown in Scheme 7. Firstly, the reduction of nitro to amino is performed at 10 bars of H₂ and 80 °C of temperature. After that, the system is depressurized, flashed out with N₂ and the reaction is continued at 140 °C and atmospheric pressure in the presence of air. The results obtained (see Scheme 7) indicate that the reduction step is almost quantitative, with complete conversion, and selectivity to 1,2-phenylenediamine higher than 95%. The following oxidation-cyclization step was performed with excellent results (98% conversion and 85% yield to **3g**). Therefore, Au/CeO₂ is a good bifunctional catalyst able to perform the one-pot three steps reaction between 1,2-dinitrobenzene and vicinal diols derivatives to give the respective quinoxaline.

4. Conclusions

Au/HT and Au/CeO₂ are excellent catalysts for the synthesis of quinoxaline derivatives of 1,2-propanediol followed by cyclocondensation with 1,2-phenylenediamine under base free conditions, at mild temperature and using air at atmospheric pressure as oxidant. The reaction network has been established being the diol **2** firstly oxidized to α -hydroxycarbonyl compound **4** (which is the controlling step) and subsequently to the dicarbonyl compound **5**. Both compounds condensate with 1,2-phenylenediamine giving the quinoxaline **3**. The oxidative cleavage of the diol is a competitive reaction which is enhanced by higher temperatures and pressures of the oxidant (air or oxygen). Au/CeO₂ can be easily recovered and reused with a small loss of activity that can be partially restored by removing the adsorbed organic material by a calcination treatment. This calcination treatment should be optimized to avoid or

decrease metal sintering. The regenerated catalyst maintains high selectivity towards 2-methylquinoxaline. With Au/HT it is more difficult to recover the initial activity after some uses.

The catalytic process presented here has been extended to different substrates (diols and 1,2-diamines derivatives), achieving good yields of the corresponding quinoxalines. Finally Au/CeO₂ allows to carry out the one-pot three steps synthesis of 2-methylquinoxaline starting from 1,2-dinitrobenzene with an excellent global yield of 83%.

5. Acknowledgements

The authors wish to acknowledge the Spanish Ministry of Education and Science for the financial support in the projects Consolider-Ingenio 2010 and CTQ-2011-27550. Generalitat Valenciana is also thanked for funding through the Prometeo program. S. M. S thanks Spanish Ministry of Education and Science for FPI fellowships.

6. References

- [1] A. Corma, S. Iborra and A. Velty, Chem. Rev. 107 (2007) 2411.
- [2] G.W. Huber, S. Iborra and A. Corma, Chem. Rev. 106 (2006) 4044.
- [3] P. Gallezot, Green Chem. 9 (2007) 295.
- [4] C.H. Christensen, J. Rass-Hansen, C. C. Marsden, E. Taarning and K. Egeblad, The renewable chemicals industry 1 (2008) 283.
- [5] J. van Haveren, E. L. Scott, J. Sanders, Biofuels Bioprod. Biorefining 2 (2008) 41.
- [6] H. Roper, Starch-Starke 54 (2002) 89.
- [7] F. W. Lichtenthaler, Chem. Res. 35 (2002) 728.
- [8] F. W. Lichtenthaler, S. C. R. Peters, Chim. 7 (2004) 65.
- [9] F. W. Lichtenthaler, Carbohydr. Res. 113 (1998) 69.
- [10] M.J. Climent, A. Corma, P. De Frutos, S. Iborra, M. Noy, A. Velty, P. Concepción, J. Catal., 269 (2010) 140.
- [11] K.M. Rapp, J. Daub, Rapp, K.M.; Daub, J in *Nachwachsende Rohstoffe: Perspektiven für die Chemie* (Hrsg.: Eggersdorfer, M; Warwel, S.; Wulff, G.), VCH, Weinheim, 1993, p. 183.
- [12] V. Lehr, M. Sarlea, L. Ott, H. Vogel, Catal. Today 121 (2007) 121.
- [13] M. Pagliaro, R. Ciriminna, H. Kimura, M. Rossi, C. D. Pina, Angew. Chem. Int. Ed. 46 (2007) 4434.
- [14] C. H. C. Zhou, J. N. Beltramini, Y. X. Fan, G. Q. M. Lu, Chem. Soc. Rev. 37 (2008) 527.
- [15] S. T. Hazeldine, L. Polin, J. Kushner, J. Paluch, K. White, M. Edelstein, E. Palomino, T. H. Corbett, J. P. Horwitz, J. Med. Chem. 44 (2001) 1758.
- [16] F. Rong, S. Chow, S. Yan, G. Larson, Z. Hong, J. Wu, Bioorg. Med. Chem. Lett. 17 (2007) 1663.

- [17] A. Jaso, B. Zarranz, I. Aldana, A. Monge, *J. Med. Chem.* 48 (2005) 2019.
- [18] R. A. Smits, H. D. Lim, A. Hanzer, O. P. Zuidelverd, E. Guaita, M. Adami, G. Coruzzi, R. Leurs, I. J. P. De Esch, *J. Med. Chem.* 51 (2008) 2457.
- [19] G. W. H. Cheeseman, E. S. G. Werstiuk, *Adv. Heterocycl. Chem.* 22 (1978) 367.
- [20] K. Yb, K. Yh, P. Jy, K. Sk, *Bioorg. Med. Chem. Lett.* 14 (2004) 541.
- [21] X. Hui, J. Desrivot, C. Bories, P.M. Loiseau, X. Franck, R. Hocquemiller, B. Fidadere, *Bioorg. Med. Chem. Lett.* 16 (2006) 815.
- [22] G. Sakata, K. Makino, Y. Karasawa, *Heterocycl.* 27 (1988) 2481.
- [23] E.D. Brock, D.M. Lewis, T.I. Yousaf, H.H. Harper, The Procter and Gamble Company USA, WO9951688 (1999).
- [24] J. L. Sessler, H. Maeda, T. Mizuno, V. M. Lynch, H. J. Furuta, *Am. Chem. Soc.* 124 (2002) 13474.
- [25] K. R. J. Thomas, M. Velusamy, J. T. Lin, C.-H. Chuen, Y.-T. Tao, *Chem. Mater.* 17 (2005) 1860.
- [26] S. Dailey, W.J. Feast, R.J. Peace, I.C. Sage, S. Till, E.L. Wood, *J. Mater. Chem.* 11 (2001) 2238.
- [27] M.J. Crossley, L.A. Johnston, *Chem. Commun.* (2002) 1122.
- [28] O. Sascha, F. Rudiger, *Synlett* (2004) 1509.
- [29] D. J. Brown, Quinoxalines Supplements II. In *The Chemistry of Heterocyclic Compounds*; Taylor, E. C., Wipf, P., Eds.; John Wiley & Sons: New Jersey, 2004.
- [30] R. S. Bhosale, S. R. Sarda, S. S. Andhapure, W. N. Jadhav, S. R. Bhusare, R. P. Pawar, *Tetrahedron Lett.* 46 (2005) 7183.
- [31] Z. Zhao, D. D. Wisnoski, S. E. Wolkenberg, W. H. Leister, Y. Wang, C. W. Lindsley, *Tetrahedron Lett.* 45 (2004) 4873.
- [32] S. V. More, M. N. V. Sastry, C. F. Yao, *Green Chem.* 8 (2006) 91.

- [33] C. Srinivas, C. N. S. S. P. Kumar, V. J. Rao, S. Palaniappan, *J. Mol. Catal. A: Chem.* 256 (2007) 227.
- [34] D. Aparicio, O. A. Attanasi, P. Filippone, R. Ignacio, S. Lillini, F. Mantellini, F. Palacios, J. M. De los Santos, *J. Org. Chem.* 71 (2006) 5897.
- [35] S. A. Raw, C. D. Wilfred, R. J. K. Taylor, *Org. Biomol. Chem.* 2 (2004) 788.
- [36] S. Y. Kim, K. H. Park, Y. K. Chung, *Chem. Commun.* (2005) 1321.
- [37] R. S. Robinson, R. J. K. Taylor, *Synlett* (2005) 1003.
- [38] S. Sithambaram, Y. Ding, W. Li, X. Shen, F. Gaenzler, S. L. Suib, *Green Chem.* 10 (2008), 1029.
- [39] S. K. Singh, P. Gupta, S. Duggineni, B. Kundu, *Synlett* 14 (2003) 2147.
- [40] S. Antoniotti, E. Duñach, *Tetrahedron Lett.* 43 (2002) 3971.
- [41] C. S. Cho, S. G. Oh, *Tetrahedron Lett.* 47 (2006) 5633.
- [42] A. Corma, *Catal. Rev.* 46 (2004) 369.
- [43] M. J. Climent, A. Corma, S. Iborra, *Chem. Sus. Chem.* 2 (2009) 500.
- [44] M. J. Climent, A. Corma, S. Iborra, *Chem. Rev.* 111 (2011) 1072.
- [45] M. J. Climent, A. Corma, S. Iborra, *RSC. Adv.* 2 (2012) 16.
- [46] D. Venu Gopal, M. Subrahmanyam, *Catal. Commun.* 2 (2001) 219.
- [47] K. V. Rao, M. Subba, M. Subrahmanyam, *Chem. Lett.* 2 (2002) 234.
- [48] T. Mallat, A. Baiker, *Catal. Today* 1994, 19, 247.
- [49] S.-I. Murahashi, N. Komiya in *Ruthenium in Organic Synthesis* (Ed.: S.-I. Murahashi), Wiley-VCH, Weinheim, 2004, p. 53.
- [50] A. Abad, P. Concepcion, A. Corma, H. Garcia; *Angew. Chem. Int. Ed.* 2005, 44, 4066.
- [51] A. Abad, C. Almela, A. Corma, H. Garcia, *Chem. Commun.* 30 (2006) 3178.
- [52] R. Juárez, A. Corma and H. Garcia, *Green Chem.* 11 (2009) 949.

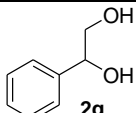
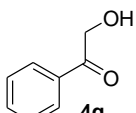
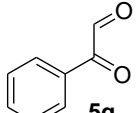
- [53] F. Cavani, A. Trifiró, A. Vaccari, *Catal. Today* 11 (1991) 173.
- [54] M. J. Climent, A. Corma, S. Iborra, L. Santos, *Chem. Eur. J.* 15 (2009) 8834.
- [55] R. G. Jacob, L. G. Dutra, C. S. Radatz, S. R. Mendes, G. Perin, E. J. Lenardao, *Tetrahedron Lett.* 50 (2009) 1495.
- [56] R. Van Hardeveld, F. Hartog, *Surf. Sci.*, 15 (1969) 189.
- [57] R. E. Benfield, *J. Chem. Soc. Faraday Trans.*, 88 (1992) 1107.
- [58] A. Corma, H. García, *Nanoparticles and Catalysis*, (2008), 389.
- [59] L. Zhang, S. A. Kozmin, *J. Am. Chem. Soc.* 126 (2004) 11806.
- [60] Q. Fu, H. Saltsburg, M. Flytzani-Stephanopoulos, *Science* 301 (2003) 935.
- [61] J. Guzman, S. Carrettin, A. Corma, *J. Am. Chem. Soc.* 127 (2005) 3286.
- [62] J. Guzman, S. Carrettin, J. C. Fierro-González, L. Hao, B. C. Gates, A. Corma, *Ang. Chem. Int. Ed.* 44 (2005) 4778.
- [63] T. Mitsudome, A. Nougima, T. Mizugaki, K. Jitsukawa, K. Kaneda, *Green Chem.* 11 (2009) 793.
- [64] T. Mitsudome, Y. Mikami, H. Funai, T. Mizugaki, K. Jitsukawa, K. Kaneda, *Angew. Chem. Int. Ed.* 47 (2008) 138.
- [65] T. Mitsudome, Y. Mikami, K. Ebata, T. Mizugaki, K. Jitsukawa, K. Kaneda, *Chem. Commun.* (2008) 4804.
- [66] K. Ebitani, K. Motokura, T. Mizugaki, K. Kaneda, *Angew. Chem. Int. Ed.* 44 (2005) 3423.
- [67] F. Rey, V. Fornés, *J. Chem. Soc. Faraday Trans.*, 88 (1992) 2223.
- [68] I. S. Nielsen, E. Taarning, K. Egeblad, R. Madsen, C. H. Christensen, *Catal. Lett.*, 116 (2007) 35.
- [69] Y. Azizi, C. Petit, V. Pitchon, *Journal of Catalysis* 256 (2008) 338.

[70] A. Corma, C. González-Arellano, M. Iglesias, F. Sánchez, *Applied Catalysis, A: General* 356 (2009) 99.

[71] A. Corma, P. Serna, *Science* 313 (2006) 332.

TABLES

Table 1. Catalytic activity of Au/CeO₂ towards **3g** formation starting from **2g**, 2-hydroxy-1-phenylethanone (**4g**) and 2-oxo-2-phenyl-acetaldehyde (**5g**).^(a)

| Entry | Reactant | time (h) | Conversion (mol%) | Selectivity to 3g ^(b) (mol%) |
|-------|--|-------------|----------------------|---|
| 1 |  2g | 24 | 97 | 72 |
| | | 2 | 42 | 75 |
| 2 |  4g | 2 | >99 | 93 |
| 3 |  5g | 5 (min) | >99 | 99 |

^(a)Reaction conditions: **1a** (0.5 mmol), **2a** (0.6 mmol), diglyme (10.5 mmol), Au/CeO₂ (4.5 wt%), **1a**/Au mol ratio = 100, at 140 °C. ^(b)As main by-products, which complete molar balance, are the following: 2-phenyl-1*H*-benzo[d]imidazole (**8**) and 1*H*-benzo[d]imidazole (**9**).

Table 2. Results of oxidation-cyclization process of **2a** with **1a** into **3a** using different catalysts.^(a)

| Entry | Catalyst | Au loading (wt%) | Molar Ratio (1a /Au) | Average size ^(b) (nm) | N _T (by np) | m (layers) | N _S (by np) | N _S (%) | r ₀ (mmol·h ⁻¹) | TOF ₁ ^(c) (h ⁻¹) | Conversion (mol%) | Yield (mol%) | Selectivity to 3a ^(d) (mol%) |
|-------|-----------------------------------|---------------------|---------------------------------|-------------------------------------|---------------------------|---------------|---------------------------|-----------------------|---|---|------------------------|-----------------|---|
| 1 | Au/CeO ₂ | 4.5 | 102 | 3.5 | 1285 | 7.8 | 459 | 36 | 0.21 | 121 | 95 | 82 | 87 |
| 2 | Au/HT | 0.7 | 129 | 3.2 | 1016 | 7.2 | 388 | 38 | 0.19 | 132 | 86 (92) ^(e) | 80 (85) | 94 |
| 3 | Au/TiO ₂ | 1.5 | 103 | 3.5 | 1330 | 7.8 | 471 | 35 | 0.04 | 23 | 39 | 36 | 92 |
| 4 | Au/Fe ₂ O ₃ | 4.5 | 99 | 3.5 | 1365 | 7.9 | 479 | 35 | 0.02 | 12 | 14 | 13 | -- |
| 5 | Au/MgO | 0.6 | 239 | 3.9 | 1840 | 8.7 | 593 | 32 | 0.02 | 36 | 20 | 18 | -- |
| 6 | Au/HTcalc ^(g) | 0.7 | 127 | 3.6 | 1448 | 8.1 | 500 | 35 | 0.12 | 91 | 71 | 68 | 96 |
| 7 | CeO ₂ | -- | -- | -- | -- | -- | -- | -- | 0.03 | -- | 22 | 18 | -- |
| 8 | HT | -- | -- | -- | -- | -- | -- | -- | 0.01 | -- | 9 | 7 | -- |

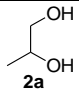
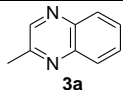
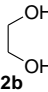
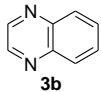
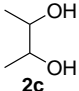
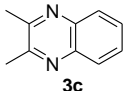
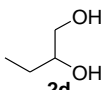
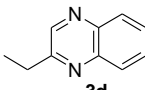
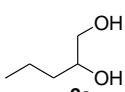
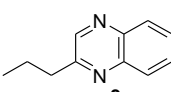
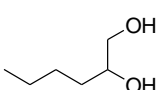
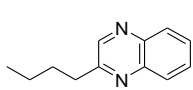
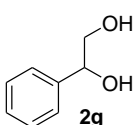
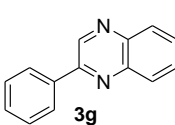
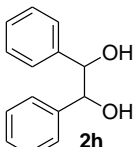
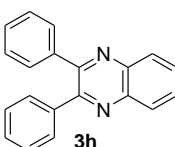
^(a)Reaction conditions: **1a** (0.5 mmol), **2a** (0.6 mmol), diglyme (10.5 mmol), 24h. ^(b)Determined by TEM. ^(c)Calculated as moles of converted **1a** divided by reaction time (0.5 h) and moles of Au in the surface (N_S). ^(d)Selectivity values at 40% conversion. As main by-products, which complete molar balance, are the following: 2-methyl-1*H*-benzo[d]imidazole (**8**) and 1*H*-benzo[d]imidazole (**9**). ^(e)Result after 30 hours. ^(f)No-nanometric CeO₂ was used as support. ^(g)Hydrotalcite calcined was used as a gold support.

Table 3. Results of oxidation-cyclization process of **2a** with **1a** into **3a** using Au/CeO₂.^(a)

| Entry | Temperature (°C) | 1a/Au (mol ratio) | time (h) | r ₀ ^(b) (mmol·h ⁻¹) | Conversion (mol%) | Selectivity to 3a ^(c) (mol%) |
|-------|---------------------|----------------------|-------------|--|----------------------|--|
| 1 | 140 | 400 | 24 | 0.12 | 67 | 94 |
| 2 | 140 | 200 | 24 | 0.16 | 85 | 89 |
| 3 | 140 | 100 | 24 | 0.22 | 95 | 87 |
| 4 | 100 | 100 | 48 | 0.09 | 47 | 98 |
| 5 | 120 | 100 | 30 | 0.15 | 69 | 97 |
| 6 | 160 | 100 | 16 | 0.26 | 99 | 77 |
| 7 | 140 ^(d) | 100 | 24 | 0.22 | 91 | 76 |
| 8 | 140 ^(e) | 100 | 24 | 0.23 | 95 | 73 |
| 9 | 140 ^(f) | 100 | 24 | 0.25 | 93 | 69 |

^(a) Reaction conditions: **1a** (0.5 mmol), **2a** (0.6 mmol), diglyme (10.5 mmol), Au/CeO₂ (4.5 wt%), **1a**/Au mol ratio = 100, at 140 °C. ^(b) Calculated as moles of converted **1a** divided by reaction time (0.5 h). ^(c) Selectivity values at 40% conversion. As main by-products, which complete molar balance, are the following: 2-methyl-1*H*-benzo[d]imidazole (**8**) and 1*H*-benzo[d]imidazole (**9**). ^(d) Experiment carried out bubbling O₂ into the reaction mixture at a constant flow rate of 0.30 mL·s⁻¹. ^(e) Experimented carried out under air pressure of 3 bars. ^(f) Experimented carried out under oxygen pressure of 3 bars.

Table 4. Influence of the diol substituents on the oxidation-cyclization process with **1a** using Au/CeO₂.^(a)

| Entry | Diol | Product | Conversion (mol%) | Yield (mol%) | Selectivity to 3a-h ^(b) (mol%) |
|-------|---|---|----------------------|-----------------|--|
| 1 |  |  | 96 | 84 | 87 |
| 2 |  |  | 99 | 91 | 92 |
| 3 |  |  | 98 | 87 | 89 |
| 4 |  |  | 96 | 81 | 85 |
| 5 |  |  | 94 | 80 | 86 |
| 6 |  |  | 99 | 81 | 82 |
| 7 |  |  | 97 | 70 | 72 |
| 8 |  |  | 99 | 35 | 35 |

^(a)Reaction conditions: **1a** (0.5 mmol), diol (0.6 mmol), diglyme (10.5 mmol), Au/CeO₂ (4.5 wt%), **1a**/Au mol ratio = 100, at 140 °C, 24 hours. ^(b)Selectivity values at 90% conversion. As main by-products, which complete molar balance, are the correspondents benzimidazoles produced from the oxidative cleavage of the diol (**8** and **9**).

Table 5. Influence of the 1,2-phenylenediamine substituent in position 4 on the oxidation-cyclization process of diamine with **2b** using Au/CeO₂.^(a)

| Entry | Reactant | Product | Conversion | Selectivity to 3a , 3i-n ^(b) | Yield |
|-------|----------|---------|------------|---|--------|
| | | | (mol%) | (mol%) | (mol%) |
| 1 | | | 99 | 92 | 91 |
| 2 | | | 90 | 78 | 70 |
| 3 | | | 92 | 80 | 73 |
| 4 | | | 91 | 83 | 75 |
| 5 | | | 97 | 88 | 86 |
| 6 | | | 95 | 84 | 81 |
| 7 | | | 99 | 89 | 88 |

^(a)Reaction conditions: diamine (0.5 mmol), **2b** (0.6 mmol), diglyme (10.5 mmol), Au/CeO₂ (4.5 wt%), **1a**/Au mol ratio = 100, at 140 °C, 24 h.

^(b)Selectivity values at 90% conversion. As main by-product, which complete molar balance is the 1*H*-benzo[d]imidazole substituted at position 6 (**9**).

FIGURES

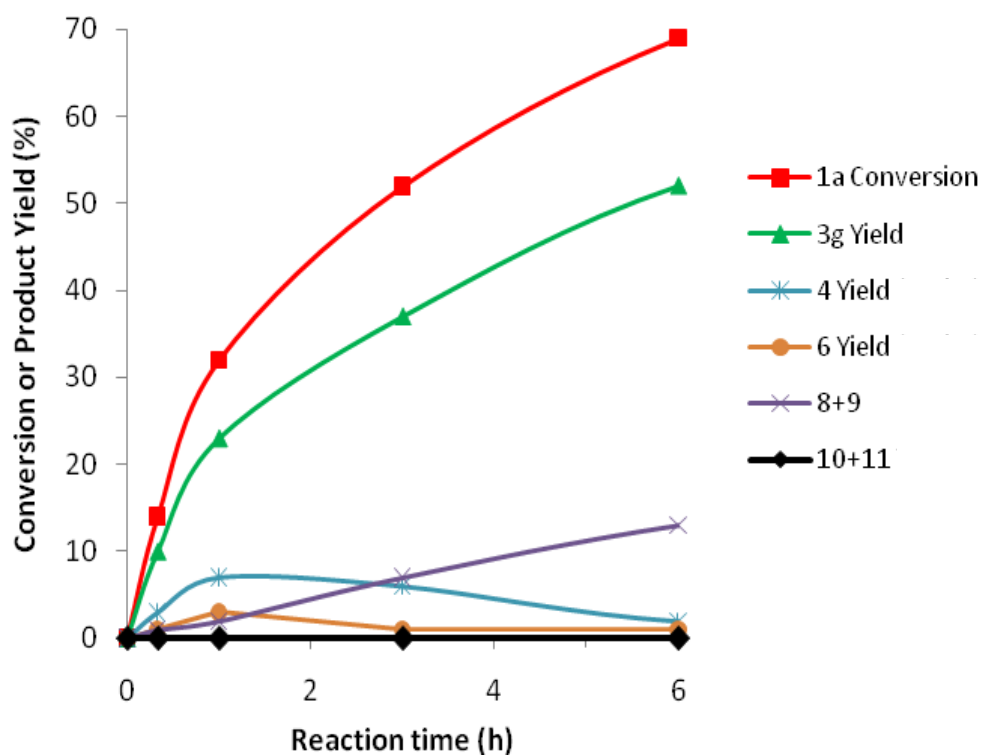


Figure 1. Kinetics plots of the different compounds (mol%) detected in the oxidation-cyclization reaction of **1a** with **2g** using Au/CeO₂. Reaction conditions: **1a** (0.5 mmol), **2g** (0.6 mmol), diglyme (10.5 mmol), Au/CeO₂ (4.5 wt%), **1a**/Au mol ratio = 100, at 140 °C.

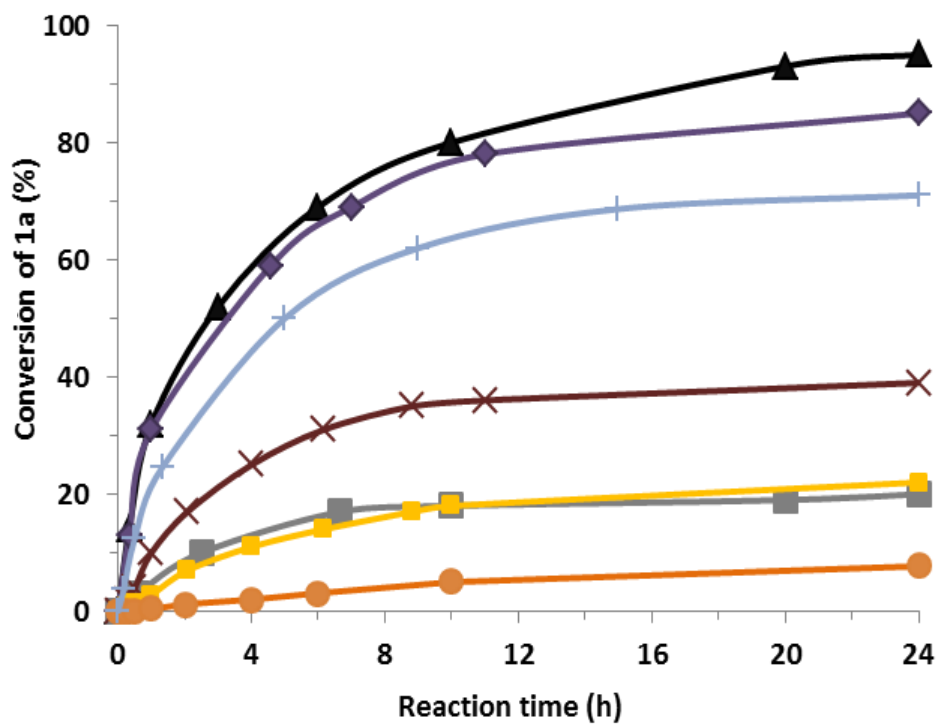


Figure 2. Conversion kinetics plots of the oxidation-cyclization of **2a** with **1a** into **3a** using different catalysts: Au/CeO₂ (▲), Au/HT (◆), Au/HTcalc (+), Au/TiO₂ (×), Au/MgO (■), CeO₂ (■) and HT (●). Reaction conditions: **1a** (0.5 mmol), **2a** (0.6 mmol), diglyme (10.5 mmol), at 140 °C.

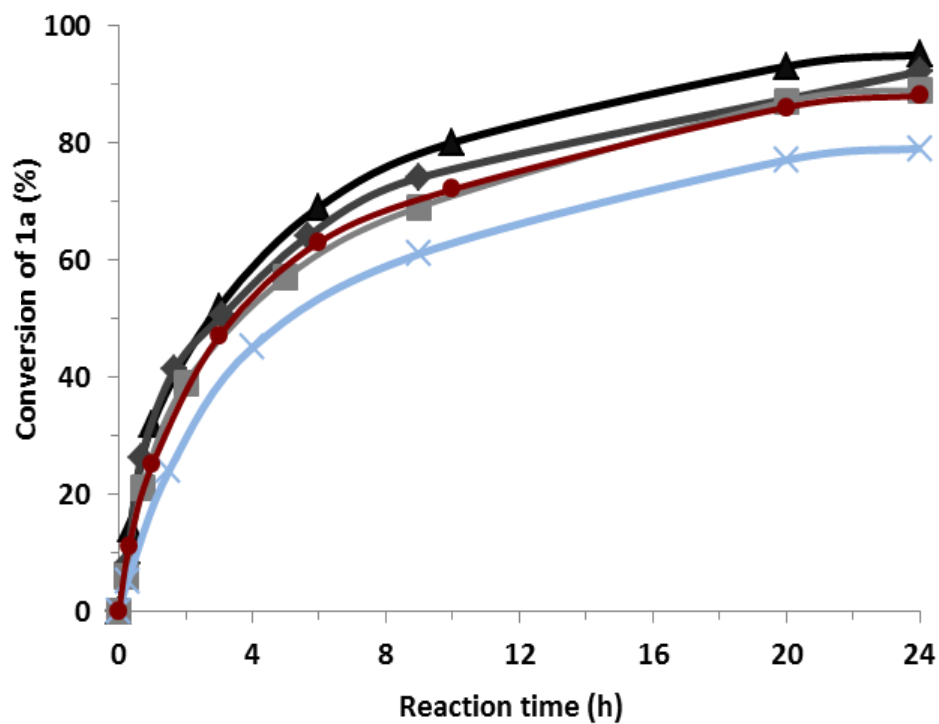


Figure 3. Conversion kinetics plots of the oxidation-cyclization of **1a** with **2a** into **3a** under successive reuses of Au/CeO₂: 1st use (▲), 2nd use (◆), 3rd use (■), 4th use (×) and 4th use after calcination (●) treatment with air at 300 °C for 10 hours. Reaction conditions: **1a** (0.5 mmol), **2a** (0.6 mmol), diglyme (10.5 mmol), at 140 °C.

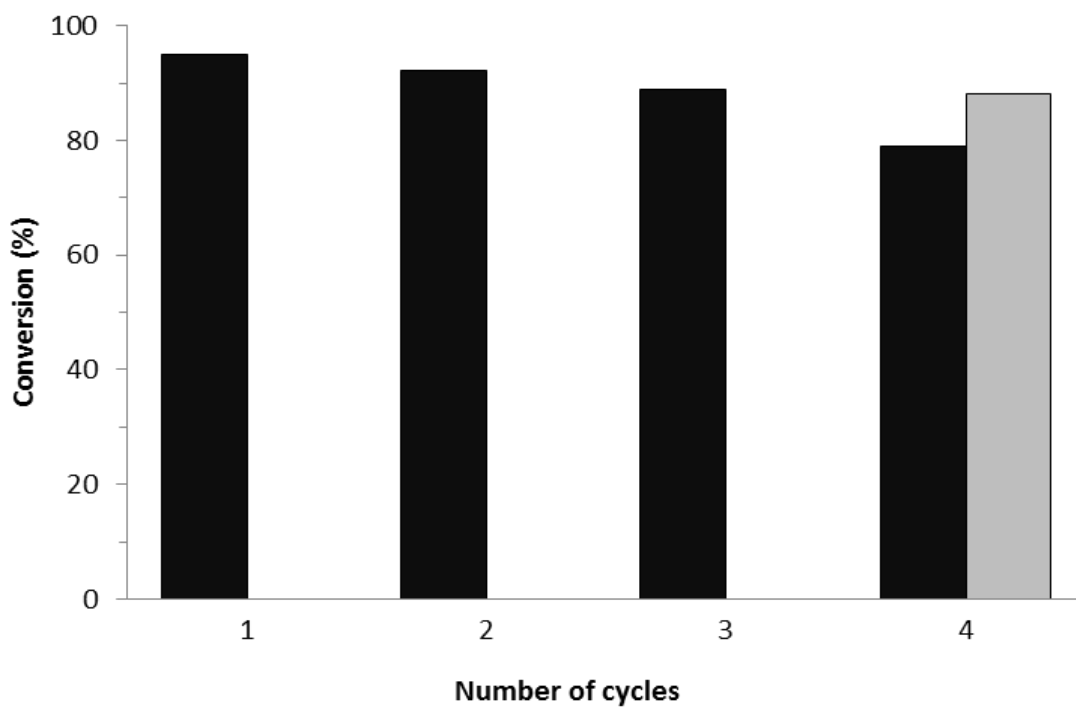


Figure 4. Conversion of **1a** with successive reuses of Au/CeO₂ in the oxidation-cyclization of **1a** with **2a** after 24 hours. In the fourth use, the bar on the right illustrates when the catalyst was used after previous treatment in air at 300 °C for 10 hours. Reaction conditions: **1a** (0.5 mmol), **2a** (0.6 mmol), diglyme (10.5 mmol), Au/CeO₂ (4.5 wt%), **1a**/Au mol ratio = 100, at 140 °C.

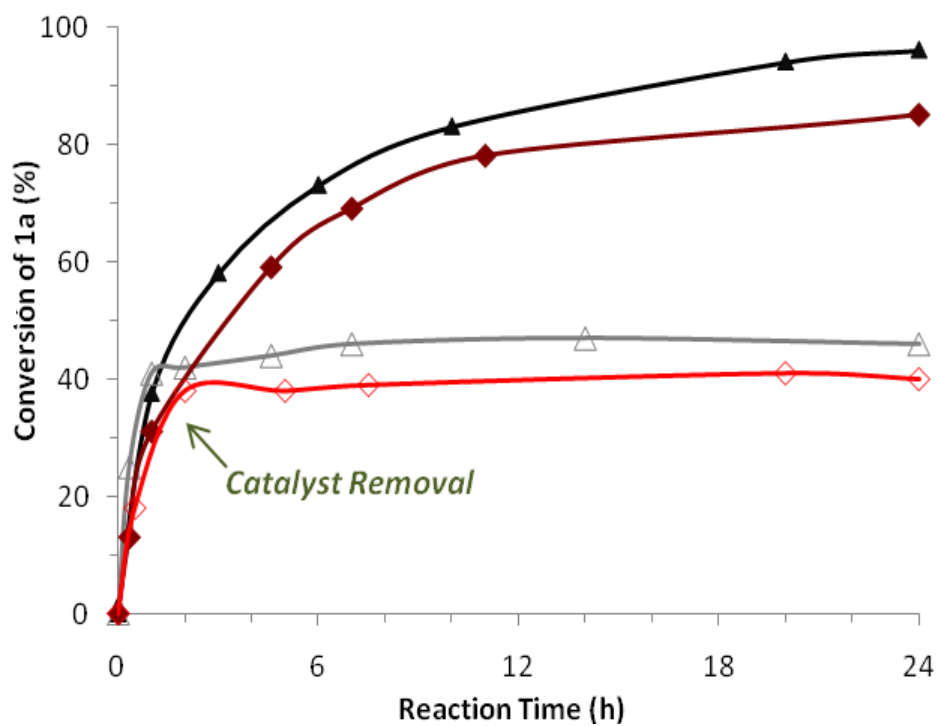


Figure 5. Conversion kinetics plots of the **1a** in the oxidation-cyclization process of **1a** with **2a** into **3a** using Au/CeO₂ (4.5 wt%) and Au/HT (0.75 wt%). Au/CeO₂'(Δ) and Au/HT'(◇) are the same experiments than Au/CeO₂(▲) and Au/HT(◆) but removing the catalyst after two hours of reaction. Reaction conditions: **1a** (0.5 mmol), **2a** (0.6 mmol), diglyme (10.5 mmol), **1a**/Au mol ratio = 100, at 140 °C.

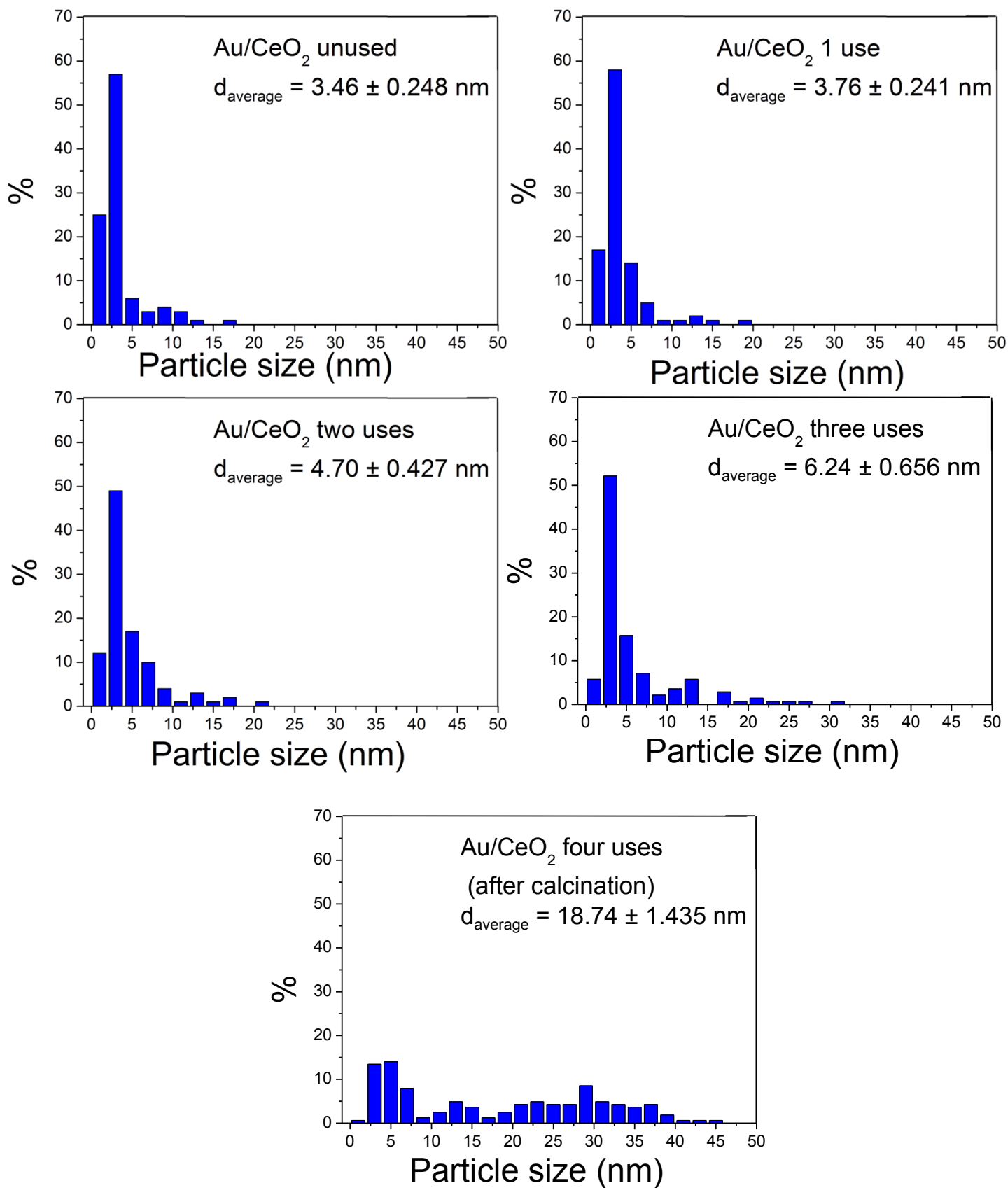


Figure 6. Gold nanoparticles size of Au/CeO₂ after several uses.

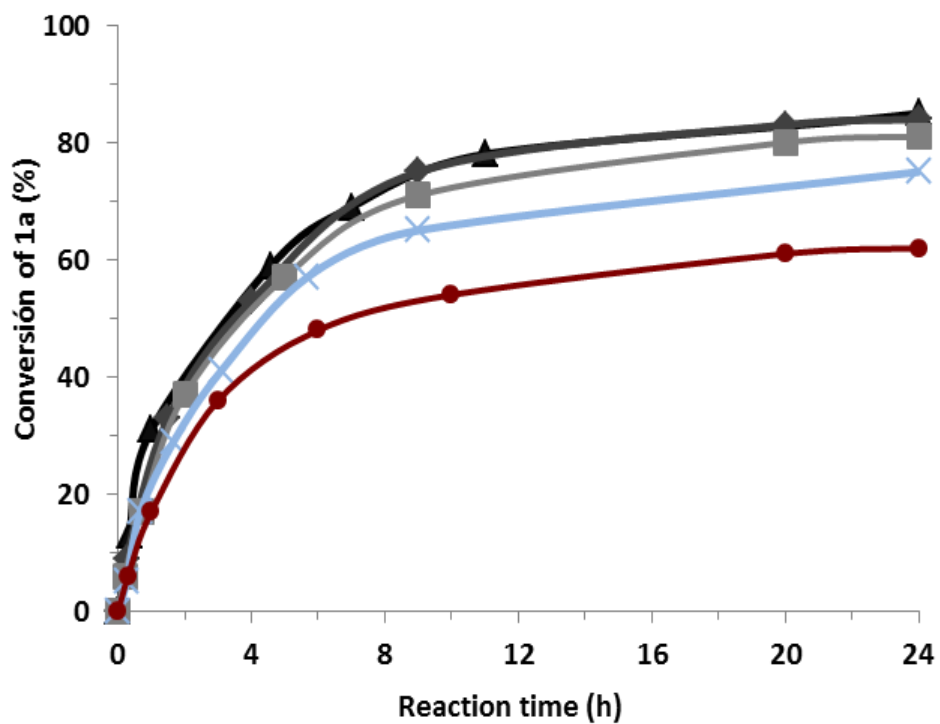


Figure 7. Conversion kinetics plots of the oxidation-cyclization of **1a** with **2a** into **3a** under successive reuses of Au/HT: 1st use (▲), 2nd use (◆), 3rd use (■), 4th use (×) and 4th use after calcination (●) treatment with air at 300 °C for 10 hours. Reaction conditions: **1a** (0.5 mmol), **2a** (0.6 mmol), diglyme (10.5 mmol), at 140 °C.

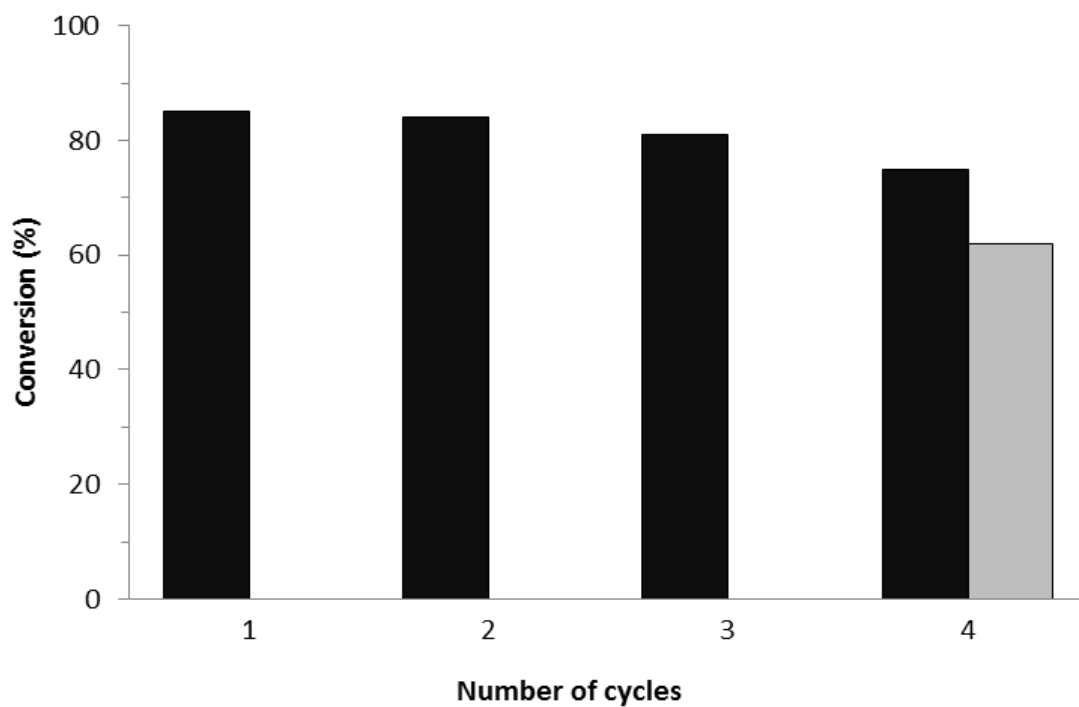


Figure 8. Conversion of **1a** with successive reuses of Au/HT in the oxidation-cyclization of **1a** with **2a** after 24 hours. In the fourth use, there are two bars because the bar on the right illustrates when the catalyst was used after previous treatment in air at 300 °C for 10 hours. Reaction conditions: **1a** (0.5 mmol), **2a** (0.6 mmol), diglyme (10.5 mmol), Au/CeO₂ (4.5 wt%), **1a**/Au mol ratio = 100, at 140 °C.

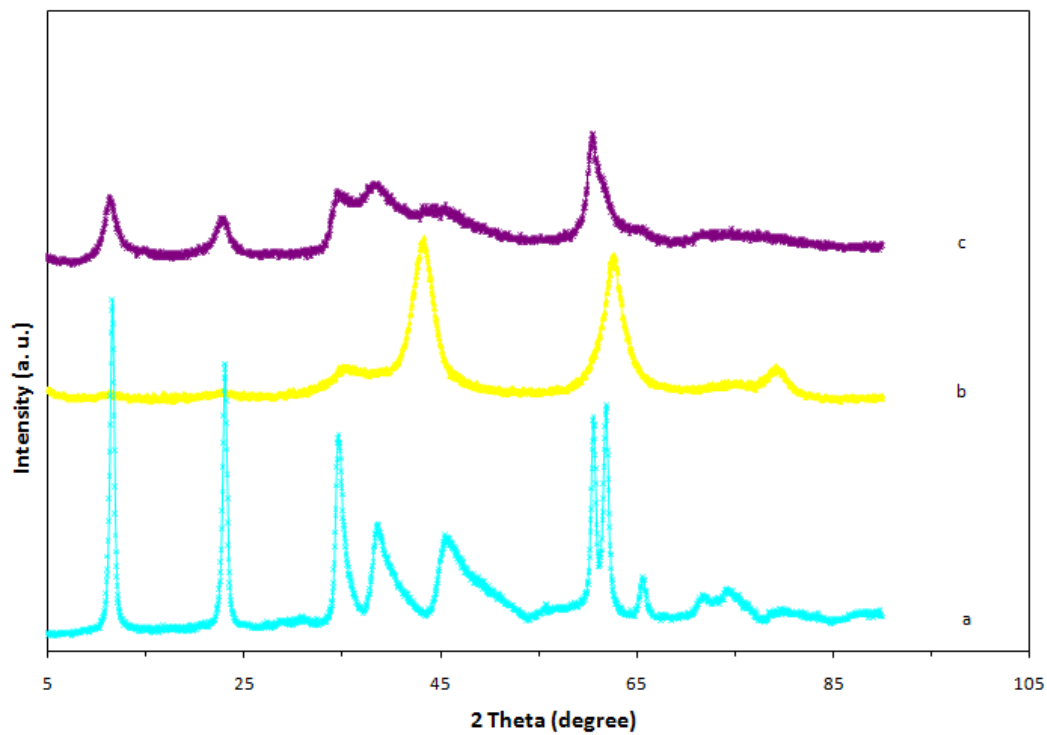


Figure 9. XRD patterns of the catalyst Au/HT under different calcination treatment: (a) Au/HT, (b) Au/HT calcined at 300 °C, (c) Au/HT calcined at 450°.

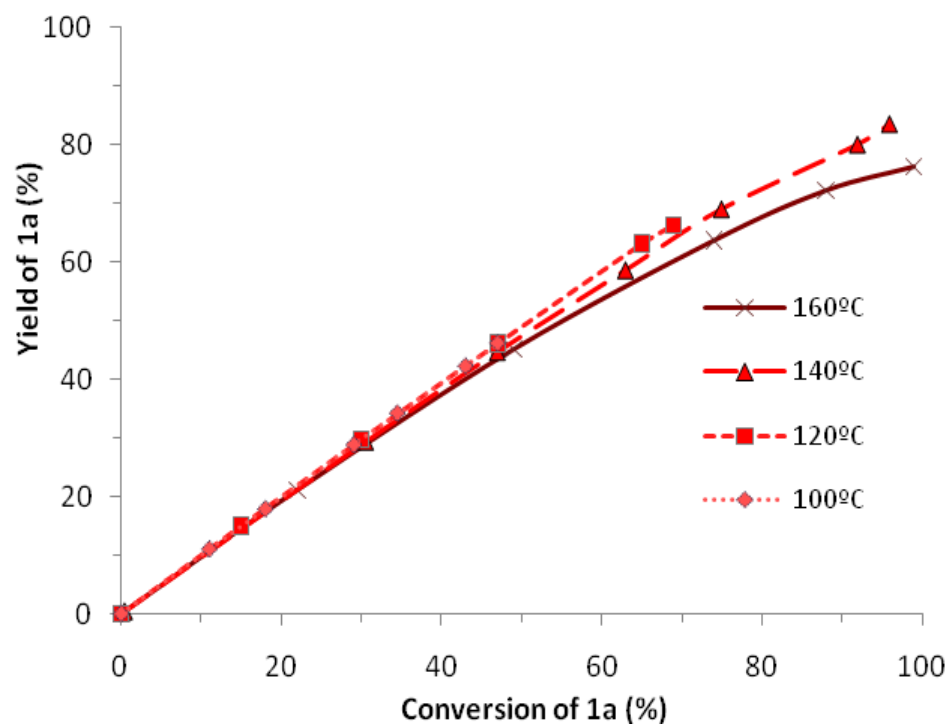
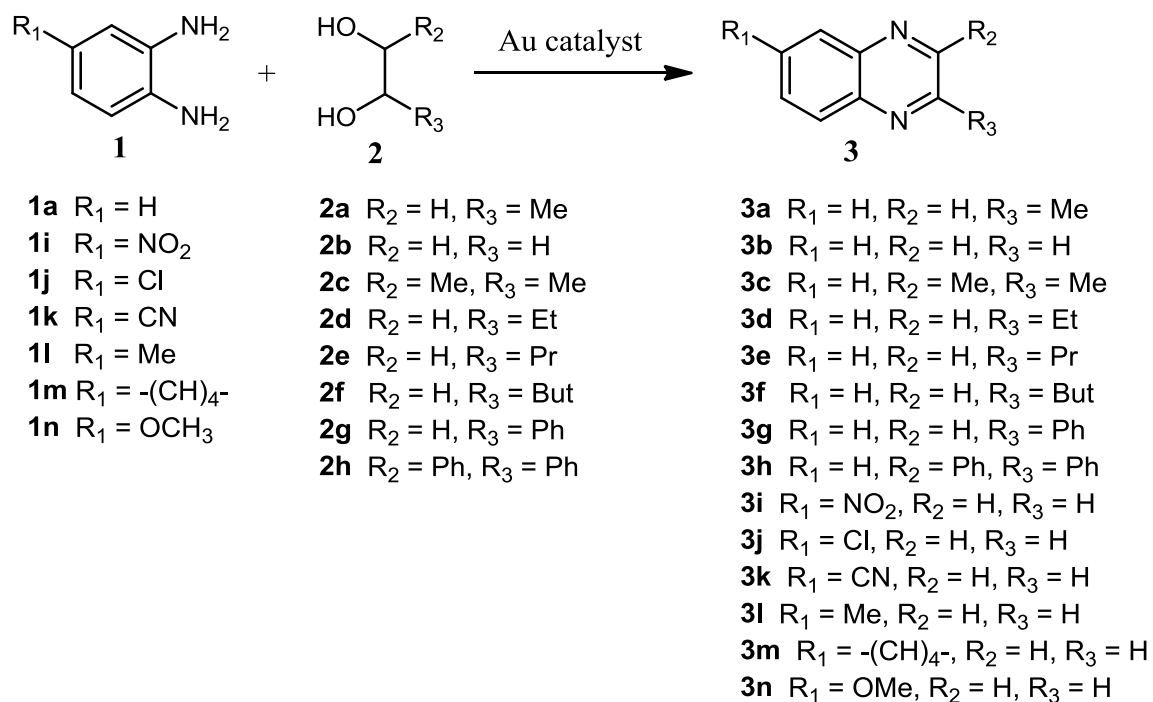
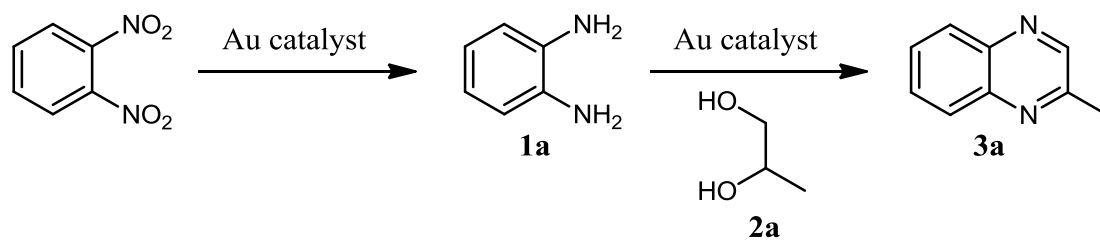


Figure 10. Effect of temperature on **3g** selectivity in the oxidation-cyclization of **1a** with **2a** using Au/CeO₂. Reaction conditions: **1a** (0.5 mmol), **2a** (0.6 mmol), diglyme (10.5 mmol), Au/CeO₂ (4.5 wt%), **1a**/Au mol ratio = 100, at 140 °C.

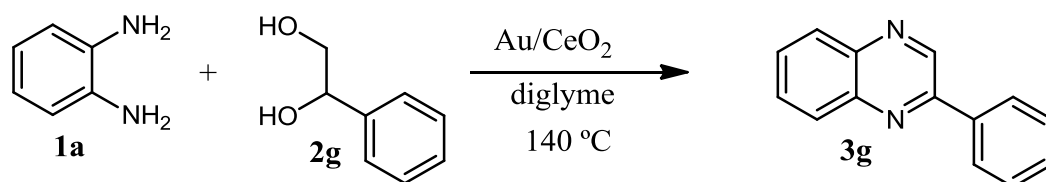
SCHEMES



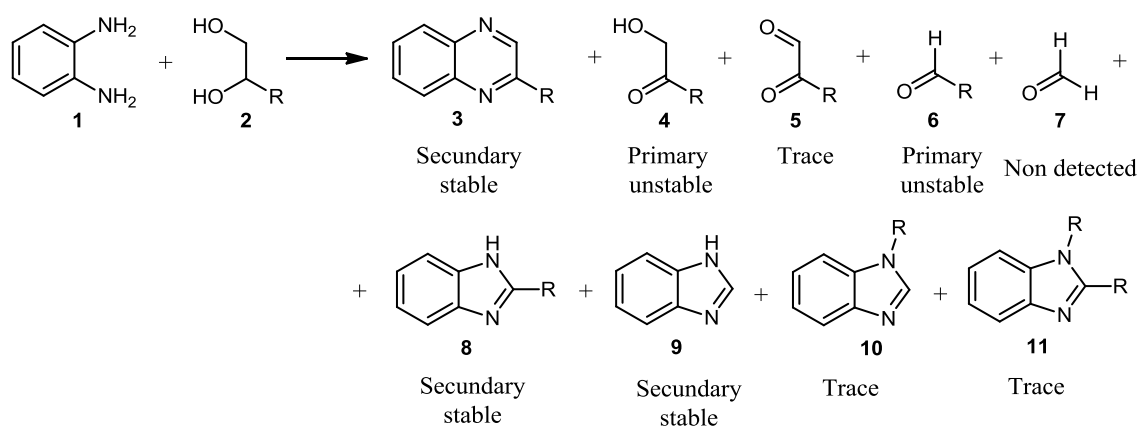
Scheme 1. Reaction pathway for the one-pot synthesis of quinoxaline derivatives.



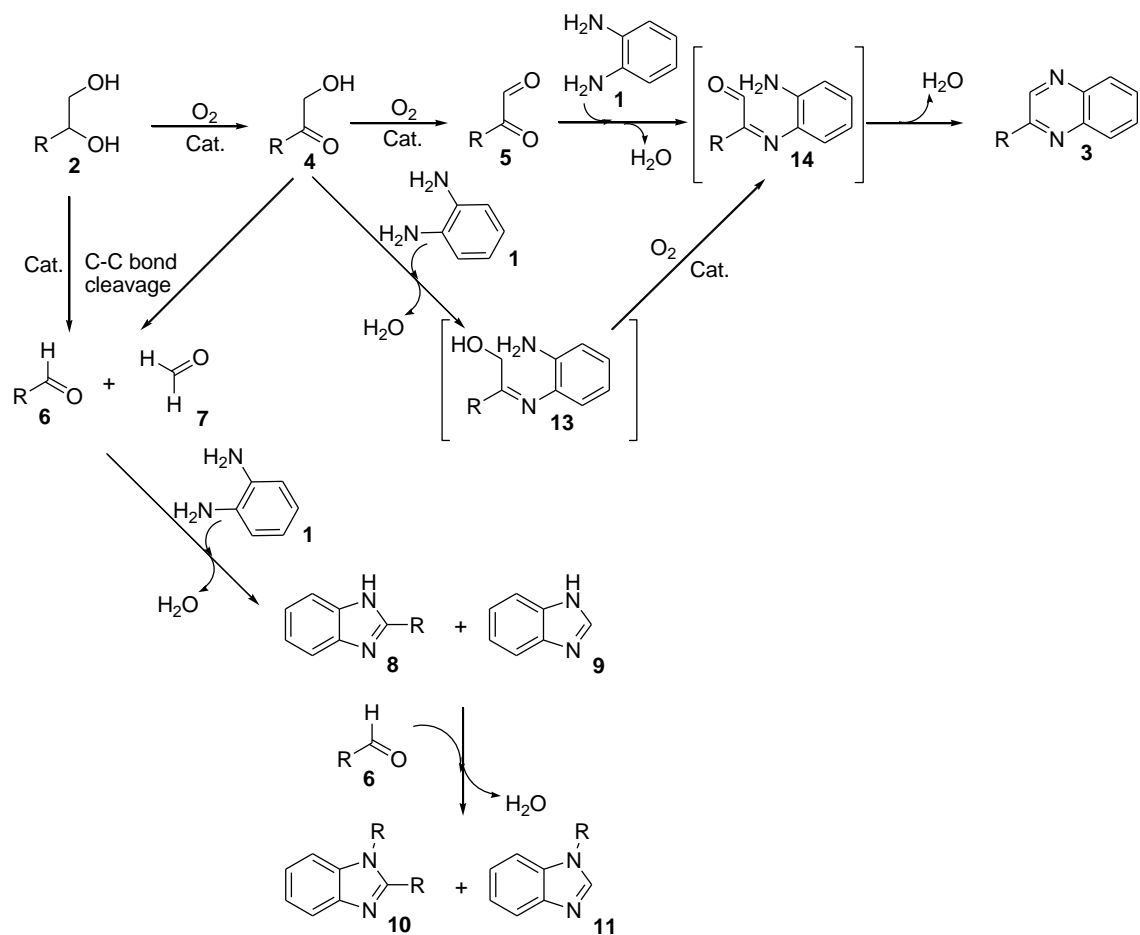
Scheme 2. Reaction pathway for the one-pot synthesis of quinoxaline derivatives.



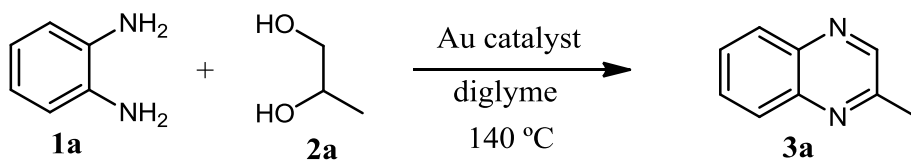
Scheme 3. Reaction pathway for the oxidation-cyclization reaction of 1a with 2g using Au/CeO₂. Reaction conditions: 1a (0.5 mmol), 2g (0.6 mmol), diglyme (10.5 mmol), Au/CeO₂ (2.4 wt%), 1a/Au mol ratio = 100, at 140 °C.



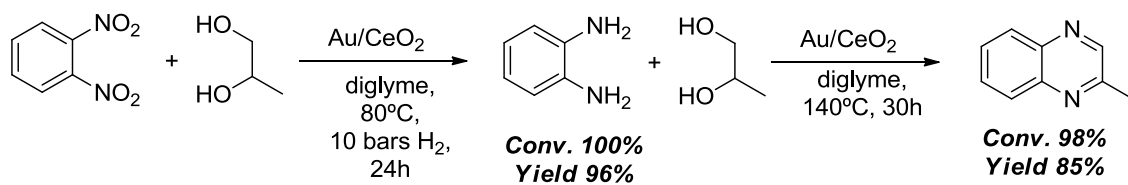
Scheme 4. Detected products in the synthesis of quinoxalines from 1,2-phenylenediamine derivatives and vicinal diols.



Scheme 5. Proposed quinoxalines synthesis mechanism from 1,2-phenylenediamine derivatives and vicinal diols.



Scheme 6. Oxidation-cyclization reaction of 1,2-phenylenediamine with 1,2-propanediol over different Au catalysts.



Scheme 7. Synthesis of 2-methylquinoxaline by one-pot reaction between 1,2-dinitrobenzene **15** and **2a** using Au/CeO₂, in 1.5 mL diglyme and mol ratio 1a/Au = 100.